

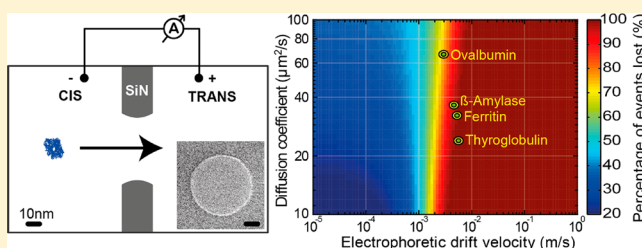
## Fast Translocation of Proteins through Solid State Nanopores

Calin Plesa,<sup>†</sup> Stefan W. Kowalczyk,<sup>†</sup> Ruben Zinsmeister,<sup>†</sup> Alexander Y. Grosberg,<sup>‡</sup> Yitzhak Rabin,<sup>§</sup> and Cees Dekker<sup>\*,†</sup><sup>†</sup>Department of Bionanoscience, Kavli Institute of Nanoscience, Delft University of Technology, Lorentzweg 1, 2628 CJ Delft, The Netherlands<sup>‡</sup>Department of Physics and Center for Soft Matter Research, New York University, 4 Washington Place, New York, New York 10003, United States<sup>§</sup>Department of Physics and Institute for Nanotechnology and Advanced Materials, Bar Ilan University, Ramat Gan 52900, Israel

## S Supporting Information

**ABSTRACT:** Measurements on protein translocation through solid-state nanopores reveal anomalous (non-Smoluchowski) transport behavior, as evidenced by extremely low detected event rates; that is, the capture rates are orders of magnitude smaller than what is theoretically expected. Systematic experimental measurements of the event rate dependence on the diffusion constant are performed by translocating proteins ranging in size from 6 to 660 kDa. The discrepancy is observed to be significantly larger for smaller proteins, which move faster and have a lower signal-to-noise ratio. This is further confirmed by measuring the event rate dependence on the pore size and concentration for a large 540 kDa protein and a small 37 kDa protein, where only the large protein follows the expected behavior. We dismiss various possible causes for this phenomenon and conclude that it is due to a combination of the limited temporal resolution and low signal-to-noise ratio. A one-dimensional first-passage time-distribution model supports this and suggests that the bulk of the proteins translocate on time scales faster than can be detected. We discuss the implications for protein characterization using solid-state nanopores and highlight several possible routes to address this problem.

**KEYWORDS:** Protein, nanopore, translocation, temporal, Smoluchowski, bandwidth



Over the past decade, nanopores have become a very popular method to study analytes at the single-molecule level. While the focus has been on nucleic acids,<sup>1,2</sup> proteins and protein DNA-complexes increasingly are becoming a prime target of investigation.<sup>3–18</sup>

There are two notable differences which make proteins more difficult to characterize than DNA by use of nanopore measurements. The well-defined structure of proteins, the source of their biological function, is normally globular, with lengths in all dimensions that are comparable to or smaller than the thickness of the pore. DNA and other polynucleotides, however, typically have one dimension much larger than the length of the pore, leading to much longer dwell times inside the nanopore compared to proteins. Second, proteins have a variety of different charges, that are distributed unevenly throughout their structure. Again, this contrasts the case for DNA which is highly negatively charged with a uniform charge distribution along its length. These differences make nanopore experiments on proteins more challenging than on DNA. This study focuses at the issues caused by the protein's short translocation times and the implications this has for characterization of proteins with solid-state nanopores.

Figure 1 shows the setup and data for a typical nanopore protein measurement. A voltage is applied across the pore,

which electrokinetically drives a protein through it, temporarily blocking the ionic current. The dynamics of the translocation process can be split into two stages, the capture step and the actual translocation through the nanopore. The former involves the biomolecule diffusing to the pore, which can be characterized by the rate at which molecules are captured. This process is governed by the diffusion constant of the analyte, assisted by the applied electric field. The rate  $J$  at which the analytes arrive at the pore entrance due to free diffusion is given by the Smoluchowski rate equation<sup>19</sup>

$$J = 2\pi c D r_p \quad (1)$$

where  $c$  is the bulk analyte concentration,  $D$  the diffusion constant, and  $r_p$  the radius of the pore. With these three values at hand, we can calculate the expected event rate based on this very well established equation.

We collected data for the event rate of a large variety of proteins<sup>3–5,7,9,20,21</sup> both from in-house experiments as well as from surveying published literature. This yielded a data set with 37 different protein-translocation experiments. It includes

**Received:** November 19, 2012

**Revised:** January 11, 2013

**Published:** January 23, 2013

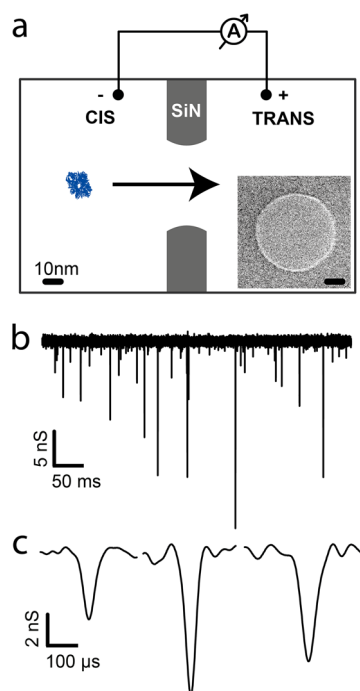


**Figure 1.** (a) Schematic illustration of the nanopore setup, with the 20 nm thick SiN membrane and a  $\beta$ -galactosidase protein shown to scale. Insert: TEM image of one of the 40 nm nanopores used in this study. (b) Current trace of  $\beta$ -galactosidase translocating through a 40 nm pore. (c) Representative translocation events, shown at better temporal resolution.

experiments on 12 different protein species conducted using SiN pores ranging in diameter from 10 to 57 nm at voltages from 50 to 200 mV. Values for the diffusion constant were determined separately for each of the protein species involved, as described in Supplementary Section S2. Figure 2 shows the ratio of the observed event rate to that predicted by Smoluchowski for this data set, as a function of the concentration multiplied by the pore radius (left plot) and of the molecular weight (right plot).

If free diffusion would govern the capture rate, we would expect a ratio of 1, irrespective of the values of  $c$ ,  $D$ , or  $r_p$ . For field-assisted captures, we even expect this ratio to be greater than 1 in all experiments due to the electrophoretic force driving the protein into the pore and thus *increasing* the capture rate. Instead we find that, while the ratio is indeed larger than 1 for dsDNA translocation, it is up to 5 orders of magnitude lower than expected for proteins, with larger and larger discrepancies for larger  $cr_p$ . When the same data is shown plotted against the molecular weight (Figure 2 right) of the particular species being measured, it becomes clear that the ratio becomes significantly lower as the size of the protein becomes smaller. Note that while the smaller proteins translocate faster and have a lower amplitude blockade due to their smaller excluded volume, it does not explain the spectacular failure of the Smoluchowski equation to describe the rate of their capture by nanopores.

How to explain this large discrepancy? Several possible explanations come to mind: (1) Adsorption<sup>5,14,17,18</sup> could explain lower capture rates, if the protein of interest would get trapped on the sidewalls of the flowcell or on the SiN membrane. To rule this out, two PMMA flowcells containing SiN membranes were incubated for one hour with 2.5  $\mu$ M BSA

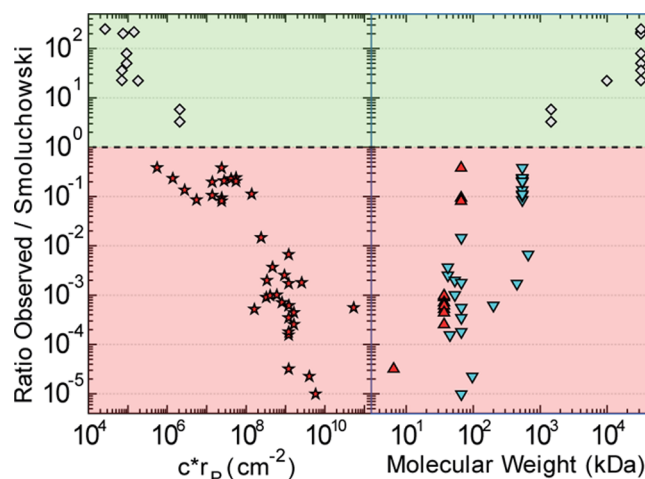


**Figure 2.** (Left) The ratio of the observed event rate to the event rate predicted by the Smoluchowski rate equation for dsDNA (white diamonds) and protein (red stars). We expect all points to be in the green area with a ratio larger than 1. Instead, we see that all protein measurements yield a ratio less than 1, with some values even up to 5 orders of magnitude smaller. This study focuses on explaining this discrepancy. (Right) Same data set versus the molecular weight. Proteins have been separated into positively charged (red triangles) and negatively charged (blue triangles) proteins. The ratio becomes worse as the size of the protein becomes smaller, which can be attributed to their faster diffusion as well as smaller excluded volumes.

or 2  $\mu$ M RecA, respectively. Subsequently, the protein solutions were recovered from the flowcells, and the protein concentration was determined using a spectrophotometer. No detectable change was observed in the bulk protein concentrations of either solution. Additionally, we modified our analysis procedure to track possible changes in the event rate over the course of the translocation experiment, expecting the observed event rate to decrease if more proteins were absorbed and the bulk concentration was lowered. Most proteins were found to exhibit a constant event rate (e.g., Figure S1). Some drop was observed for Avidin, which had its event rate steadily lowered, until becoming less than half its initial value after 20 min (Supplementary Section S3). While this shows that adsorption may sometimes be a contributing factor in devices in which the ratio of surface to volume is not negligible, its effect is too small to explain the low event rates observed. (2) Aggregation of the proteins might be another contributing factor, but it is unlikely to be a dominant effect, given the large number of different protein species and the broad range of concentrations tested. Moreover, dynamic-light-scattering measurements of the hydrodynamic radius for several of the proteins showed no evidence of aggregation. (3) Electroosmosis is known to play an important role in protein translocation of nanopores and can even be responsible for the translocation of proteins occurring at a polarity opposite to what is expected from simple electrostatics.<sup>3</sup> For typical pH values used in these experiments, from 7 to 8, the SiN surface of the pore is known to be negatively charged,<sup>3</sup> with a magnitude that depends on a number of factors, particularly the SiN membrane treatment. For negatively charged protein, the electroosmotic force opposes the translocation of the proteins. The fact, however, that very low event rates are also observed for positively charged proteins, which are aided by the electroosmotic force, rules this out as the primary source of the event rate discrepancy. (4) One might question our

assumption that the capture process is diffusion-controlled. Indeed, barrier-limited capture was previously reported in protein capture into small pores.<sup>9,11</sup> However, we focus our study on large (>10 nm) nanopores with diameters much larger than the protein size, and we observe no evidence (such as exponential voltage dependence) of barrier-limited transport.

Finally, (5) a possible explanation is the finite temporal resolution in nanopore experiments. Indeed, we conclude that limited temporal resolution is the most likely explanation for the anomalously low event rates observed in virtually all nanopore probing experiments on proteins. The idea is that proteins move through the nanopore so swiftly that they escape detection. The limited temporal resolution can be attributed to two sources. First, the bandwidth of the amplifier. The commonly used Axon Axopatch 200B amplifier has a bandwidth of about 52 kHz.<sup>22</sup> Second, the signal-to-noise ratio (SNR) of the translocation events is limited, and recorded signals are filtered to distinguish events from the noise inherently present in the system. This distorts the shape of the events with a duration shorter than twice the rise time of the filter used ( $T_r = 0.332/\text{BW}$  for a Gaussian low pass filter (LPF)), which lowers their amplitude and can significantly increase the apparent dwell time.<sup>18</sup> This is illustrated in Figure 3a, where rectangular pulses with durations from 200 to 10  $\mu\text{s}$  are filtered with a 10 kHz Gaussian LPF. If an event has a duration sufficiently below  $2T_r$ , equal to 66  $\mu\text{s}$  in this case, its amplitude drops below the detection level, the analysis software treats it as noise, the protein translocation is not noticed, and the event rate is underestimated. We investigated this effect for thyroglobulin (660 kDa), one of the proteins used in the experimental section of this work (Supplementary Section S6). The expected conductance blockade was determined using its excluded volume, as others have done in the past.<sup>4,5,12,15</sup> Pulses with this conductance blockade and ranging in duration from 1 to 100  $\mu\text{s}$  were then filtered to determine the minimum detectable pulse duration for the characteristic noise level in our pores. The minimum detectable pulse duration (MDPD) was estimated to be 25  $\mu\text{s}$ , which is larger than the 20  $\mu\text{s}$  temporal resolution of our amplifier. Since the MDPD becomes larger as proteins become smaller, we conclude that the SNR is nearly always the limiting factor setting the temporal resolution. In other words, the smaller the protein is, the more events we will miss as they are shorter than the MDPD. This implies that we should observe a decrease in the event rate with decreasing protein size, as indeed is observed in Figure 2 (right panel).

We now quantitatively estimate how many events are lost due to the finite temporal resolution. We do so using the first-passage time distribution (FPTD) for one-dimensional diffusion as derived for nanopores by Talaga and Li.<sup>11</sup> This model provides the probability that a protein with an electrophoretic drift velocity  $v$ , set by the voltage drop across the pore, will translocate with a given dwell time  $t$ , as detailed in Supplementary Section S5. This was used to generate dwell time distributions for various values of the diffusion constant and electrophoretic drift velocity. Four of these distributions, corresponding to four of the proteins used in the experimental part of our study, are shown in Figure 3b. For each of these proteins diffusion constants are determined using the method of He and Niemeyer.<sup>23</sup> This involves using the molecular weight and radius of gyration as correlation parameters to determine the diffusion constant. The electrophoretic drift velocities of the proteins were estimated based on their Stokes radii and their net charge, as determined from zeta-potential

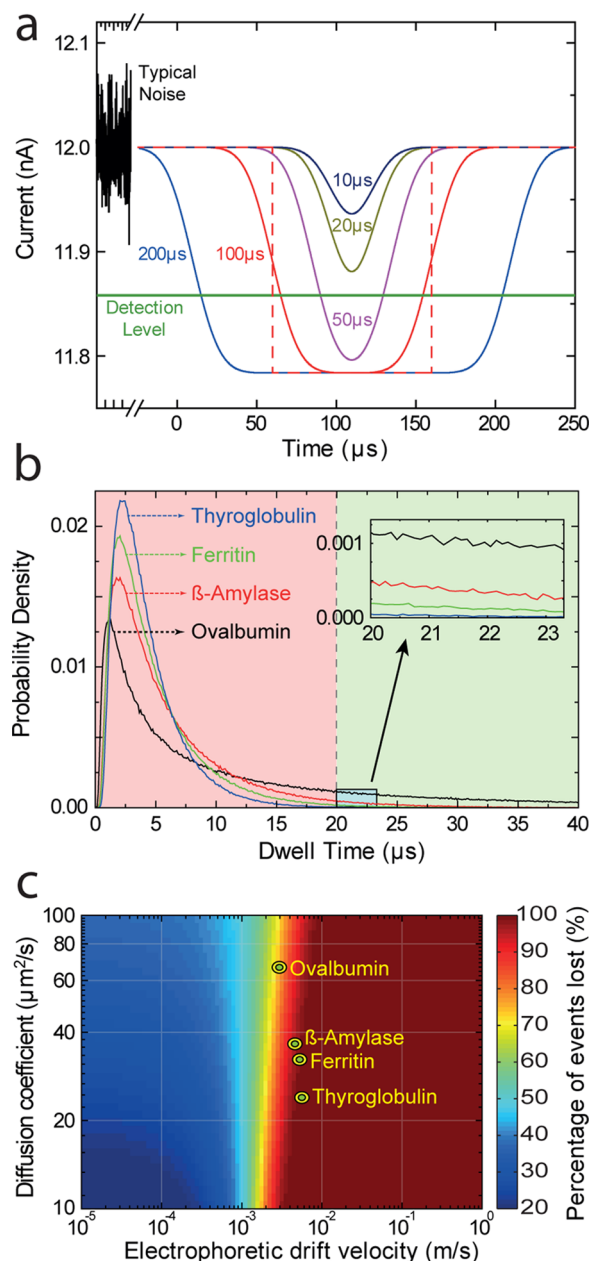


**Figure 3.** (a) The distortion of rectangular pulses of 10–200  $\mu\text{s}$  duration by a 10 kHz Gaussian filter. For a 100  $\mu\text{s}$  pulse duration the dashed red line shows an ideal pulse (delayed 40  $\mu\text{s}$  for visual clarity), before filtering, while the solid red line shows the same 100  $\mu\text{s}$  pulse after filtering. All pulses have the same amplitude before filtering. Due to the limited rise time of the filter, any pulse with a duration less than twice the filter rise time ( $2T_r = 66 \mu\text{s}$ ) is distorted. (b) A simulated dwell-time histogram showing visible (green) and lost (red) events given a resolution limit of 20  $\mu\text{s}$ . At this resolution we expect the smallest protein, ovalbumin, to show the most events (insert). If the temporal resolution would be improved to below 6  $\mu\text{s}$ , however, the largest protein, thyroglobulin, would produce the most observable events. (c) The percentage of events below the temporal resolution (color scale) for various values of the diffusion coefficient and electrophoretic drift velocity. The estimated positions of four proteins are shown. We expect the majority of events for these proteins to be lost.

measurements<sup>24</sup> that we carried out on these proteins (Supplementary Section S4). As Figure 3b displays, the analysis reveals that smaller proteins (e.g., ovalbumin) have a most



probable dwell time which is smaller compared to the larger proteins (e.g., thyroglobulin), but the tail of their distribution is larger. Counterintuitively, therefore, smaller proteins can therefore yield more detectable events. This effect is expected to reverse as the temporal resolution of the system becomes smaller than  $6\ \mu\text{s}$  which however is smaller than the temporal resolution of commercial amplifiers. The amount of events lost for a particular protein is set by its size, net charge, and the minimum time resolvable by the system. The fraction of events below the temporal resolution (set as  $20\ \mu\text{s}$ ) within the typical range of values for the diffusion constant and the electrophoretic drift velocity is shown in Figure 3c. As the positions of the proteins on this diagram show, the vast majority of protein translocations will not be observed under normal conditions. This suggests that any events that are observed either belong to the far tail of the dwell time distribution or are held long enough inside the pore due to protein–pore interactions to be resolved.

To experimentally verify that the limited temporal resolution is the cause of the discrepancy observed, the event rate dependence was investigated separately for each of the parameters in the Smoluchowski rate equation. The dependence on the diffusion constant was studied by translocating five proteins (aprotinin 6.5 kDa, ovalbumin 45 kDa,  $\beta$ -amylase 200 kDa, ferritin 450 kDa, thyroglobulin 660 kDa) of varying size, each at a concentration of  $1\ \mu\text{M}$ , through a 40 nm SiN pore, in 1 M NaCl with pH 7.5, at an applied voltage of 50 mV. Based on Smoluchowski's equation as well as our FPTD simulation, one would expect the event rate to increase with increasing  $D$ , since proteins should be able to diffuse to the pore entrance faster. Experimentally, however, we see just the opposite, as shown in Figure 4a: the event rate decreases as the size of the protein becomes smaller, and  $D$  thus grows. The observed decrease must be attributed to the decrease in the SNR as the proteins get smaller (Figure S5b). Aprotinin, the smallest protein tested, had an event rate within the noise floor of the system. This noise floor of false positives is determined by the rate of noise peaks with sufficient amplitude to be detected as apparent events and is estimated to be between 0.3 and 0.5 Hz for our system (Supplementary Section S7). The noise floor is shown in the panels of Figure 4 as a light red area at the bottom, except in panel b where it has been omitted for visual clarity. To test the dependence of the rate on the pore-diameter, a large 540 kDa protein at 46 nM concentration,  $\beta$ -Galactosidase, and a small 37 kDa protein at  $1.35\ \mu\text{M}$  concentration, human chorionic gonadotropin (hCG) were translocated through pores varying in diameter from 5 to 40 nm, as shown in Figure 4b. The event rate increased linearly with pore diameter for the large  $\beta$ -galactosidase, as predicted by Smoluchowski. But the event rate for hCG remained low and relatively constant, indicating non-Smoluchowski behavior. Finally, the concentration dependence for these two proteins was investigated, by applying increasingly concentrated solutions to a flow cell containing a 20 nm pore, as shown in Figure 4c. Again,  $\beta$ -galactosidase followed the expected Smoluchowski behavior, whereas the hCG's event rate remained within the noise floor of the system. In an attempt to investigate the dependence of an increased SNR for the hCG, we also checked  $J$  for two concentrations with a 5 nm pore (light blue data points in Figure 4c), but we did not observe any difference in behavior. By further increasing the hCG concentration, we finally did observe the event rate rise above the noise floor at very high concentrations above  $1\ \mu\text{M}$ .

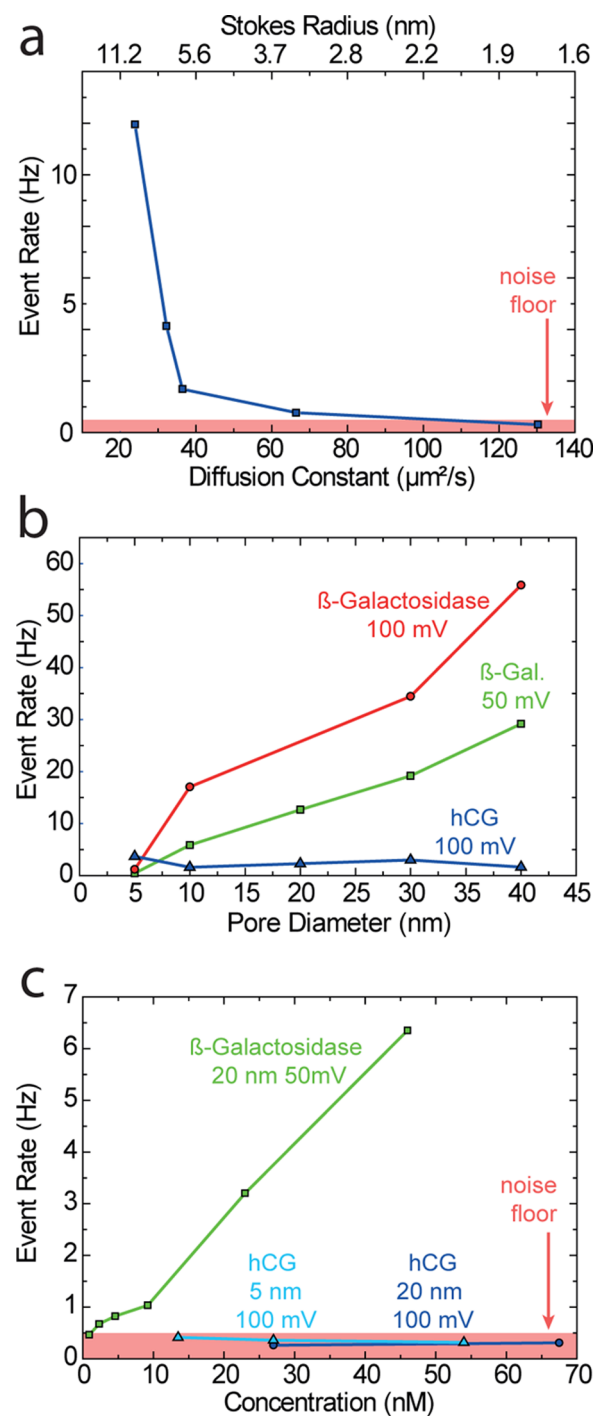


**Figure 4.** (a) The event rate of protein translocation through a 40 nm nanopore for aprotinin (6.5 kDa), ovalbumin (45 kDa),  $\beta$ -amylase (200 kDa), ferritin (450 kDa), and thyroglobulin (660 kDa) at  $1\ \mu\text{M}$  concentration. The event rate is observed to decrease as the protein becomes smaller, that is, when the diffusion constant becomes larger. This is counter to the predictions by both Smoluchowski and the FPTD model and is attributed to the reduction in the SNR as the proteins become smaller. (b) The pore-size dependence of the event rate for 46 nM 540 kDa  $\beta$ -galactosidase and  $1.35\ \mu\text{M}$  37 kDa hCG. The event rate of  $\beta$ -galactosidase increases linearly with pore size, as expected, while no change is observed for hCG. (c) The concentration dependence of the event rate for these proteins. The event rate of  $\beta$ -galactosidase increases linearly with concentration, as predicted by Smoluchowski. The event rate of hCG remains within the noise floor for all measurements.

What are the implications and possible solutions to this issue of a very significantly reduced event rate for protein translocation through nanopores? The findings presented in this study suggest that most of the protein translocation events that are observed are either due to protein–pore interactions or represent the far tail of the residence-time distribution. In patch-clamp techniques, analysis software such as Qub<sup>25</sup> routinely takes into account events that are missed due to limited temporal resolution in the estimation of kinetic parameters, but this has, to our knowledge, so far not been incorporated for nanopores. Some previous studies<sup>26,27</sup> have attributed low event rates in small antibiotic molecules translocating through membrane pores to limited temporal resolution. Additionally this subject has been touched upon briefly in the past for protein translocation through solid state nanopores.<sup>3,9,11,15</sup> If nanopores are to be used in biosensors, one requirement would be the ability to determine the concentration of analyte in the sample being probed. Given the high percentage of lost events, which also varies widely with protein mass and charge, it seems unlikely that this can be achieved without significant technological improvements.

Solutions to address this temporal issue can be divided into two categories: (i) slowing down the speed of the biomolecules, or (ii) improving the bandwidth of the amplifier utilized. Traditionally the former approach has involved altering buffer properties such as the viscosity or the temperature, both of which have the drawback of simultaneously reducing the amplitude of the signal.<sup>28</sup> For dsDNA, it has been shown that an 18 K drop in temperature can increase the dwell time by 1.7× while decreasing the conductance blockade by 1.5×.<sup>28</sup> Similarly, increasing the viscosity by 4.4× can increase the dwell time by 3.7× while reducing the signal by 2.2×.<sup>28</sup> In the case of proteins, the pH of the buffer can be modified to be close to the isoelectric point of the protein being studied. This will slow down the translocation velocity by reducing the charge of the protein.<sup>15</sup> Alternatively, the protein of interest can be immobilized within the detection volume of the pore for long periods of time using either surface modification<sup>29–31</sup> of the pore or designed DNA-origami structures inserted into the pore.<sup>32,33</sup> Both of these approaches implement a bait and prey type system. More recently, Yusko et al.<sup>12</sup> have demonstrated an elegant technique which involves coating the nanopore sidewalls with a fluidic lipid bilayer and anchoring the target analyte to the bilayer. Both Yusko et al. and others<sup>34</sup> have shown that the diffusion of these anchored analytes is dominated by the in-plane diffusion constant of the lipids, which is 2 orders of magnitude smaller than the typical diffusion constant for proteins in free solution. As this approach does not modify the inner measurement channel, there is no loss in signal. The second possible solution involves improving the electronics of the system, to directly measure the translocation signal at higher bandwidth. Several low-noise high-bandwidth amplifier designs have been proposed in the past few years.<sup>35–38</sup> Some of these have been designed specifically for use with nanopores and have been demonstrated to allow measurements on short DNA oligos that have previously been invisible. Assuming we apply one of these amplifiers, say with a bandwidth of 1 MHz, to our protein measurements, our FPTD model predicts that, for a temporal resolution of 1 μs, we would expect to observe most proteins and only 6% of events to be lost. Unfortunately, however, the increased bandwidth comes with an increase in noise at the higher frequencies, so realistically this will be difficult to

achieve. As previously noted, the temporal resolution is limited by the SNR, meaning that the best resolution will occur in experiments with large proteins, small pores, and low-noise membranes.

While all of these methods may help improve the number of translocation events visible, none of these solutions seem to completely address the problem at hand. It is thus clear that the issues discussed in this paper will remain a problem for protein translocation experiments with nanopores well into the foreseeable future.

## ■ ASSOCIATED CONTENT

### ■ Supporting Information

Materials and methods, experimental translocation data, tracking of event rate changes, protein charge measurements, FPTD model details, and filtering effects. This material is available free of charge via the Internet at <http://pubs.acs.org>.

## ■ AUTHOR INFORMATION

### Corresponding Author

\*E-mail: [c.dekker@tudelft.nl](mailto:c.dekker@tudelft.nl).

### Notes

The authors declare no competing financial interest.

## ■ ACKNOWLEDGMENTS

We would like to thank Christophe Danelon and Aleksei Aksimentiev for productive discussions, as well as Khin Sam Ly for contributions to nanopore measurements. This work was funded in part by the European Research Council research grant NanoforBio (no. 247072).

## ■ REFERENCES

- (1) Dekker, C. *Nat. Nanotechnol.* **2007**, 2 (4), 209–215.
- (2) Venkatesan, B. M.; Bashir, R. *Nat. Nanotechnol.* **2011**, 6 (10), 615–624.
- (3) Firnkes, M.; Pedone, D.; Knezevic, J.; Döblinger, M.; Rant, U. *Nano Lett.* **2010**, 10, 2162–7.
- (4) Fologea, D.; Ledden, B.; McNabb, D. S.; Li, J. *Appl. Phys. Lett.* **2007**, 91, 539011–539013.
- (5) Han, A.; Schürmann, G.; Mondin, G.; Bitterli, R. A.; Hegelbach, N. G.; de Rooij, N. F.; Staufer, U. *Appl. Phys. Lett.* **2006**, 88, 093901.
- (6) Kowalczyk, S. W.; Hall, A. R.; Dekker, C. *Nano Lett.* **2009**, 10 (1), 324–328.
- (7) Kowalczyk, S. W.; Kapinos, L.; Blosser, T. R.; Magalhaes, T.; van Nies, P.; LimRoderick, Y. H.; Dekker, C. *Nat. Nanotechnol.* **2011**, 6 (7), 433–438.
- (8) Ledden, B.; Fologea, D.; Talaga, D. S.; Li, J. *Proteins* **2011**, 129–150.
- (9) Oukhaled, A.; Cressiot, B.; Bacri, L.; Pastoriza-Gallego, M.; Betton, J.-M.; Bourhis, E.; Jede, R.; Gierak, J.; Auvray, L.; Pelta, J. *ACS Nano* **2011**, 5, 3628–38.
- (10) Sexton, L. T.; Horne, L. P.; Sherrill, S. a.; Bishop, G. W.; Baker, L. a.; Martin, C. R. *J. Am. Chem. Soc.* **2007**, 129, 13144–52.
- (11) Talaga, D. S.; Li, J. *J. Am. Chem. Soc.* **2009**, 131, 9287–97.
- (12) Yusko, E. C.; Johnson, J. M.; Majd, S.; Prangkio, P.; Rollings, R. C.; Li, J.; Yang, J.; Mayer, M. *Nat. Nanotechnol.* **2011**, 6, 253–60.
- (13) Spiering, A.; Getfert, S.; Sischka, A.; Reimann, P.; Anselmetti, D. *Nano Lett.* **2011**, 11 (7), 2978–2982.
- (14) Freedman, K. J.; Jülgens, M.; Prabhu, A.; Ahn, C. W.; Jemth, P.; Edel, J. B.; Kim, M. *J. Anal. Chem.* **2011**, 83 (13), 5137–5144.
- (15) Han, A.; Creus, M.; Schürmann, G.; Linder, V.; Ward, T. R.; de Rooij, N. F.; Staufer, U. *Anal. Chem.* **2008**, 80, 4651–8.
- (16) Stefureac, R.; Trivedi, D.; Marziali, A.; Lee, J. S. *J. Phys.: Condens. Matter* **2010**, 22 (45), 454133.

- (17) Niedzwiecki, D. J.; Grazul, J.; Movileanu, L. *J. Am. Chem. Soc.* **2010**, *132* (31), 10816–10822.
- (18) Pedone, D.; Firnkes, M.; Rant, U. *Anal. Chem.* **2009**, *81*, 9689–94.
- (19) Smoluchowski, M. v. *Z. Phys. Chem.* **1917**, *92*, 129.
- (20) Chen, P.; Gu, J.; Brandin, E.; Kim, Y.-R.; Wang, Q.; Branton, D. *Nano Lett.* **2004**, *4* (11), 2293–2298.
- (21) Merchant, C. A.; Healy, K.; Wanunu, M.; Ray, V.; Peterman, N.; Bartel, J.; Fischbein, M. D.; Venta, K.; Luo, Z.; Johnson, A. T. C.; Drndic, M. *Nano Lett.* **2010**, *10* (8), 2915–2921.
- (22) Uram, J. D.; Ke, K.; Mayer, M. *ACS Nano* **2008**, *2*, 857–72.
- (23) He, L.; Niemeyer, B. *Biotechnol. Prog.* **2003**, *19* (2), 544–548.
- (24) Winzor, D. J. *Anal. Biochem.* **2004**, *325* (1), 1–20.
- (25) Qin, F.; Auerbach, A.; Sachs, F. *Biophys. J.* **1996**, *70* (1), 264–280.
- (26) Mahendran, K.; Chimerel, C.; Mach, T.; Winterhalter, M. *Eur. Biophys. J.* **2009**, *38* (8), 1141–1145.
- (27) Mahendran, K.; Singh, P. R.; Arning, J.; Stolte, S.; Kleinekathöfer, U.; Winterhalter, M. *J. Phys.: Condens. Matter* **2010**, *22* (45), 454131.
- (28) Fologea, D.; Uplinger, J.; Thomas, B.; McNabb, D. S.; Li, J. *Nano Lett.* **2005**, *5*, 1734–7.
- (29) Ali, M.; Ramirez, P.; Tahir, M. N.; Mafe, S.; Siwy, Z.; Neumann, R.; Tremel, W.; Ensinger, W. *Nanoscale* **2011**, *3* (4), 1894–1903.
- (30) Iqbal, S. M.; Akin, D.; Bashir, R. *Nat. Nanotechnol.* **2007**, *2* (4), 243–248.
- (31) Wei, R.; Gatterdam, V.; Wieneke, R.; Tampe, R.; Rant, U. *Nat. Nanotechnol.* **2012**, *7* (4), 257–263.
- (32) Bell, N. A. W.; Engst, C. R.; Ablay, M.; Divitini, G.; Ducati, C.; Liedl, T.; Keyser, U. F. *Nano Lett.* **2012**, *12* (1), 512–517.
- (33) Wei, R.; Martin, T. G.; Rant, U.; Dietz, H. *Angew. Chem., Int. Ed.* **2012**, *51* (20), 4864–4867.
- (34) Zhang, L.; Dammann, K.; Bae, S. C.; Granick, S. *Soft Matter* **2007**, *3* (5), 551–553.
- (35) Ferrari, G.; Farina, M.; Guagliardo, F.; Carminati, M.; Sampietro, M. *Electron. Lett.* **2009**, *45*, 1278.
- (36) Ferrari, G.; Gozzini, F.; Molari, A.; Sampietro, M. *IEEE J. Solid-State Circuits* **2009**, *44* (5), 1609–1616.
- (37) Rosenstein, J.; Ray, V.; Drndic, M.; Shepard, K. L. *Circuit Des.* **2011**, 59–62.
- (38) Uddin, A.; Yemenicioglu, S.; Chen, C.-H.; Corgliano, E.; Milaninia, K.; Xia, F.; Plaxco, K.; Theogarajan, L. *Proc. SPIE, Biosens. Nanomed. V* **2012**, *8460*, 846010.